

Weighing massive neutrinos with Lyman- α observations

Anjan Kumar Sarkar^{2†} and Shiv K. Sethi^{1‡}

¹Raman Research Institute, C. V. Raman Avenue, Sadashivnagar, Bengaluru 560080, India

²National Centre for Radio Astrophysics, TIFR, Pune University Campus, Post Bag 3, Pune 411 007, India.

E-mail: †asarkar@ncra.tifr.res.in, ‡sethi@rri.res.in

Abstract. The presence of massive neutrinos has still not been revealed by the cosmological data. We consider a novel method based on the two-point line-of-sight correlation function of high-resolution Lyman- α data to achieve this end in the paper. We adopt semi-analytic models of Lyman- α clouds for the study. We employ Fisher matrix technique to show that it is possible to achieve a scenario in which the covariance of the two-point function nearly vanishes for both the spectroscopic noise and the signal. We analyze this near 'zero noise' outcome in detail to argue it might be possible to detect neutrinos of mass range $m_\nu \simeq 0.05\text{--}0.1\text{ eV}$ with signal-to-noise of unity with a single QSO line of sight. We show that this estimate can be improved to $\text{SNR} \simeq 3\text{--}6$ with data along multiple line of sights within the redshift range $z \simeq 2\text{--}2.5$. Such data sets already exist in the literature. We further carry out principal component analysis of the Fisher matrix to study the degeneracies of the neutrino mass with other parameters. We show that Planck priors lift the degeneracies between the neutrino mass and other cosmological parameters. However, the prospects of the detection of neutrino mass are driven by the poorly-determined parameters characterizing the ionization and thermal state of Lyman- α clouds. We have also mentioned the possible limitations and observational challenges posed in measuring the neutrino mass using our method.

Contents

1	Introduction	1
2	Correlating Lyman-α observations	2
3	Fisher matrix	4
3.1	Choice of parameters	6
4	Summary and Conclusions	10
A	Appendix A: Covariance of the Estimator	13

1 Introduction

In the past few decades, neutrino oscillation experiments have established that standard model neutrinos are massive. In particular, these experiments measure mass differences between the three neutrinos and detect two eigenstates of non-zero masses: $\Delta m_{32}^2 = (2.43 \pm 0.13) \times 10^{-3} \text{ eV}^2$ and $\Delta m_{21}^2 = (7.59 \pm 0.21) \times 10^{-5} \text{ eV}^2$ (for details see e.g. [1–4]). The smaller mass difference is between electron and muon neutrinos and the larger mass difference is between the tau and either electron or muon neutrinos. These two mass differences do not allow one to determine the hierarchy of masses. If tau neutrino is more massive (Normal hierarchy), the sum of the three masses $\sum_i m_\nu^i > 0.045 \text{ eV}$. If electron/muon neutrinos are more massive (Inverted hierarchy), then $\sum_i m_\nu^i > 0.09 \text{ eV}$.

It is well known that massive neutrinos have important implications for cosmology—light, massive neutrinos constitute hot dark matter (HDM) in the universe. Unlike the particle physics data which only provides a lower limit on the sum of masses the cosmological observables are sensitive to the total mass. From CMB and galaxy clustering data it is clear that the dominant component of the dark matter is cold dark matter (CDM) (e.g. [5] and references therein). Massive neutrinos provide a sub-dominant HDM component to the matter content of the universe. In the past decade, a number of studies have placed constraints on the total neutrino mass $\sum m_\nu$ using different observational probes. Planck CMB temperature and polarization data along with CMB lensing reconstruction yields the following constraint the HDM component: $\sum_i m_\nu^i < 0.27 \text{ eV}$. The constraint improves with the inclusion of low-redshift BAO data: $\sum_i m_\nu^i < 0.12 \text{ eV}$ ([5]). A further improvement, $\sum_i m_\nu^i < 0.09 \text{ eV}$, has been reported following the inclusion of the redshift-space distortion analyses of the SDSS-IV eBOSS survey [6]. (All the upper limits quoted above are at 95% confidence level.)

The CMB and low-redshift galaxy clustering data are sensitive to scales $k \lesssim 0.2 \text{ Mpc}^{-1}$. Lyman- α data can potentially probe Jeans’ scales in intergalactic medium in the redshift range $2.0 < z < 6$: $k \lesssim 5 \text{ Mpc}^{-1}$. However, the analysis of Lyman- α data yield weaker bounds $\sum m_\nu^i < 0.5 \text{ eV}$ (e.g. [7, 8] use both high-spectral resolution Lyman- α data from XQ-100 and HIRES/MIKE and low-resolution data from BOSS) largely owing to uncertainty in thermal and dynamical state of Lyman- α clouds, which is degenerate with cosmological parameters (for a detailed discuss see e.g. [8]). The joint analysis of Lyman- α data with Planck CMB and galaxy data significantly improves the constraint: $\sum_i m_\nu^i < 0.09 \text{ eV}$ [8]. From this discussion it is clear that no single cosmological probe can give requisite constraints

on the sum of neutrino masses. While CMB anisotropies and large-scale structure observations probe similar scales, a combination of the two is needed. CMB anisotropy measurement is based on angular projection of linear scales (it is sensitive to $k \simeq \ell/\eta_0$ where $\eta_0 = \int_0^{t_0} dt/a$ is the conformal time at the present) which washes out information of perturbations at smaller scales. This situation is partly alleviated by large-scale clustering (e.g. BAO) data, but this data needs supplementary information from CMB data (e.g. prior information on parameters such as n_s and $\Omega_m h^2$ which are determined very precisely by the CMB data). The Lyman- α data is sensitive to much smaller scales and hence it is potentially a better probe but it also needs precise information on cosmological parameters from CMB and galaxy data to be an effective probe of neutrino masses (e.g. [9–13]).

The current study focuses on Lyman- α data as a probe of massive neutrinos. Our approach relies on semi-analytic modelling of Lyman- α clouds. Lyman- α observations measure the contrast of background QSO fluxes as a function of the observing frequency. Our statistical estimator correspond to the two-point correlation function of the flux contrast in frequency (redshift) space. This function captures information about massive neutrinos through the suppression of three-dimensional matter power spectrum in the presence of massive neutrinos. Using Fisher matrix method, we take into account both the detector noise and the cosmic variance owing to the signal. Our statistical estimator allows multiple probes of the underlying three-dimensional power spectra. The most interesting is the one in which the covariance of the two-point correlation function of both the spectroscopic noise and the signal could nearly vanish. We investigate the implications of this 'zero noise' situation in detail. In addition, we assess the impact of priors on both cosmological parameters from CMB data and parameters that determine the thermal and dynamical state of the clouds on the signal-to-noise of the detection of neutrino mass. Finally, we carry out principal component analysis of the Fisher matrix to understand the degeneracy of the extracted quantity (the neutrino mass) with other parameters.

In the next section, we briefly summarize the semi-analytic method and derive the one-dimensional correlation function. The covariance of the correlation function for both the signal and the noise is derived in Appendix A. Next we introduce the Fisher matrix for our observational setting, explain the choice of parameters, and present our main results. The final section is reserved for the summary of our main results and concluding remarks. Throughout this paper, we use the bestfit parameters of the spatially flat model as estimated with the Planck CMB data [5].

2 Correlating Lyman- α observations

Lyman- α clouds are absorption features observed along the line of sights to high-redshift quasars (blueward of the Lyman- α peak in quasar spectra). These absorption features are caused by neutral hydrogen in regions of mildly non-linear baryonic density contrast (e.g. [14]). These observations measure the flux decrement in the observed quasar spectrum δ_F . We further define: $\delta_F = (F - \bar{F})/\bar{F}$, where F and \bar{F} are the observed and continuum fluxes of the observed quasar. δ_F is a function of distance along the line of sight and hence, can be expressed as a function of redshift. The Lyman- α clouds have HI column densities in the range $N_{\text{HI}} \simeq 5 \times 10^{12} - 10^{15} \text{ cm}^{-2}$ and temperature $T \simeq 10^4 \text{ K}$. These clouds become optically thick to Lyman- α photons for $N_{\text{HI}} \gtrsim 10^{14} \text{ cm}^{-2}$. The distribution of HI in Lyman- α clouds trace baryonic density fluctuations. Under the assumption that the baryon number density $n_b(z)$ at a given redshift z follows a lognormal distribution [15, 16], the baryon number density

bears the following relation with the baryon density contrast $\delta_b(z)$:

$$n_b(z) = n_0(z) \exp(\delta_b - \langle \delta_b^2 \rangle / 2) \quad (2.1)$$

where $\delta_b(z)$ follows the Gaussian distribution and $n_0(z) = \langle n_b(z) \rangle$ gives the mean baryon number density of the IGM at redshift z .

At any given redshift,

$$\begin{aligned} \delta_F(z) &= [\exp(-\tau) - 1] \\ &= \sum_{i=1}^{\infty} \frac{(-1)^i}{i!} \tau^i. \end{aligned} \quad (2.2)$$

Here $\tau(z)$ is the optical depth of Lyman- α clouds. From Lyman- α data and their calibration against hydrodynamical simulations that has been used to model the thermal and dynamical state of the clouds, it is possible to write $\tau(z)$ as,

$$\tau(z) = A(z) \left(\frac{n_b}{n_0} \right)^\beta, \quad (2.3)$$

where $\beta = 2 - 0.7(\gamma - 1)$; γ is the semi-adiabatic index for the Lyman- α clouds that has values in the range $1 \leq \gamma \leq 1.6$, and $A(z)$ can be expressed as, [17–20]

$$A(z) = 0.946 \left(\frac{1+z}{4} \right)^6 \left(\frac{\Omega_b h^2}{0.022} \right)^2 \left(\frac{T_0}{10^4 \text{K}} \right)^{-0.7} \left(\frac{J}{10^{12} \text{s}^{-1}} \right)^{-1} \left(\frac{H(z)}{H_0} \right)^{-1}. \quad (2.4)$$

Using Eqs. (2.3) and (2.1), it is possible to write the optical depth $\tau(z)$ in terms of the underlying baryon density field $\delta_b(z)$. This formalism allows one to treat large values of both the density contrast $\delta_b(z)$ and the optical depth $\tau(z)$. In our work we only consider large density contrast and only the linear term in the expansion given by Eq. (2.2). We note that this means only a subset of data such that $\tau < 1$ is included in the analysis. This means either analysing only the low redshift data (Eq. (2.3)) and/or excluding Lyman- α clouds with $N_{\text{HI}} \gtrsim 10^{14} \text{cm}^{-2}$ from the analysis ¹ The high spectral-resolution Lyman- α data shows that only a small fraction of Lyman- α clouds are optically thick for $z \lesssim 2.5$ (e.g. [21]). This information is also captured in the effective optical depth, τ_{eff} : $\tau_{\text{eff}} \lesssim 0.2$ at $z \lesssim 2.5$ (e.g. [22]). This shows that only a small fraction of data needs to be excluded for $z \lesssim 2.5$. Our proposed estimator, two-point correlation function in redshift space, is not biased by the missing data (for details of estimating two-point function for the case of missing data see e.g. [23, 24] and references therein).

The assumption that $\tau < 1$ further allows us to express the two-point correlation function of the flux contrast (Eq. (2.2)) as:

$$\mathcal{C}_{FF}(z_a, z_b) \equiv \langle \delta_F(z) \delta_F(z') \rangle = \langle \tau(z_a) \tau(z_b) \rangle = A^2 \times e^{(\beta^2 - \beta)\xi(0)} \times e^{\beta^2 \xi_{ab}} \quad (2.5)$$

Here $\xi(\Delta z)$ is the 2-point correlation function of $\delta_b(z)$:

$$\xi(\Delta z) = \langle \delta_b(z) \delta_b(z') \rangle, \quad (2.6)$$

¹It should be noted that this is the only way to linearly relate the observable (flux contrast) to the underlying density field (optical depth) and would be applicable not just for the semi-analytic approach we adopt here. It is possible to use the transition from $\tau < 1$ to $\tau > 1$ in redshift space to constrain density field of the underlying cosmological model [19, 20].

$\Delta z = |z - z'|$ gives the absolute magnitude of the separation between redshifts z and z' , and $\xi(0) = \langle \delta_b(z)\delta_b(z) \rangle$, gives the RMS of the baryon density field $\delta_b(z)$.

The two-point correlation function of $\delta_b(z)$ for a given redshift separation Δz is computed using one-dimensional baryon power spectrum $P_{1D}(k_{1D}, z)$ as,

$$\xi(\Delta z) = \frac{1}{2\pi} \int_{-\infty}^{\infty} P_{1D}(k_{1D}, z) e^{ik_{1D}r'_z \Delta z} dk_{1D}, \quad (2.7)$$

where $r'_z = dr_z/dz$ denotes the 1st derivative of the comoving distance at the redshift z . The one-dimensional baryon power spectrum $P_{1D}(k_{1D}, z)$ can be computed using the three-dimensional matter power spectrum $P_m(k, z)$ as,

$$P_{1D}(k_{1D}, z) = \frac{1}{2\pi} \int_{|k_{1D}|}^{\infty} \frac{P_m(k', z)}{[1 + (k'/k_J)^2]^2} k' dk'. \quad (2.8)$$

at a redshift z . The three-dimensional power spectrum is obtained from the publicly available code CAMB².

We also compare the numerical results with the fitting formula provided by [25], that allows one to include massive neutrinos. We find that the two approaches agree within a few percent for parameters of interest to us. We assume Planck bestfit parameters for our study for a spatially flat universe. In Figure 1, we show the one-dimensional baryonic correction function (Eq. (2.7)) and the the impact of massive neutrinos on the correlation function. The Jeans wavenumber, k_J , can be expressed as:

$$k_J = \frac{1}{H_0} \left[\frac{2\gamma k_B T_0}{3\mu m_p \Omega_m (1+z)} \right]^{-1/2}. \quad (2.9)$$

The other symbols used above have their usual meaning. Eq. (2.8) accounts for the suppression in the baryon power spectrum in redshift range of interest.³

The covariance of the flux contrast correlation function is also of interest to us here. This function is derived in Appendix A for both the signal and spectroscopic noise.

3 Fisher matrix

The aim of this paper is to study the feasibility of the detection of massive neutrinos using the Lyman- α data. We first discuss the data needed for our purposes. We consider each quasar line-of-sight to be of length $\Delta z = 0.2$, which corresponds to a comoving length $r \simeq 200$ Mpc at $z = 2-3$. To reliably estimate the flux contrast, the continuum level F_0 needs to be modelled accurately. This requires the flux contrast to be detected with high S/N at finer spectral resolution. For Lyman- α clouds such that $\tau < 1$, the absorption line is unsaturated with a thermal velocity width $\simeq 10$ km sec⁻¹ (for $T \simeq 10^4$ K). We assume the spectral resolution to be $\Delta v = 5$ km sec⁻¹ to avoid line blanketing. This corresponds to $\delta z \simeq 5 \times 10^{-5}$ at

²lambda.gsfc.nasa.gov/toolbox/camb_online.html

³Two assumptions made here need re-stating: (a) $P_m(k, z)$ is also the power spectrum of baryonic gas because baryonic perturbations follow dark matter perturbation in linear theory for the redshift range of interest, (b) we assume the baryonic power is suppressed below the Jeans scale k_J at a given redshift. However, this suppression also depends on the redshift evolution of the gas at higher redshifts. If the gas got reionized at $z \simeq 7.5$, as Planck results suggest [5] and the universe remained ionized at smaller redshifts, the suppression could be different from our assumption but doesn't affect our main results.

$z = 2$. This yields nearly 5000 independent spectral resolution elements with length scale range 0.05–200 Mpc (Day et al. [21] present a sample of 87 high-resolution intermediate-redshift QSOs in the redshift range $2 < z < 5$. The pixel for their sample corresponds to $\simeq 2.1 \text{ km sec}^{-1}$. The S/N per pixel is close to ten and $S/N \simeq 19.5$ per resolution element. Our envisaged theoretical setting correspond closely to the spectral resolution and S/N of these QSOs).

With this observational setting, we next define the Fisher matrix based on two-point correlation function along the line of sight. Fisher matrix provides us an estimate of the precision with which it will be possible to measure the parameters used to model a given observation. The Fisher matrix F_{ij} for the parameter set λ_i is computed as (e.g. [26]):

$$F_{pq} = \sum_{abcd} [\mathcal{C}^{FF}(z_a, z_b)]_{,p} [\text{COV}(z_a, z_b; z_c, z_d)]^{-1} [\mathcal{C}^{FF}(z_c, z_d)]_{,q}, \quad (3.1)$$

where a, b, c, d denote indices for individual redshifts i.e. z_a . The indices p and q denote derivatives with respect to parameters λ_i . The sum in Eq. (3.1) is over all pairs such that $\Delta z = |z_a - z_b| = |z_c - z_d|$. $\text{COV}(z_a, z_b; z_c, z_d)$ gives the covariance of the two-point correlation function $\mathcal{C}_{FF}(z_a, z_b)$.

The covariance of the two-point correlation function $\text{COV}(z_a, z_b; z_c, z_d)$ receives contribution from both the signal and spectroscopic noise and is derived in appendix A (Eqs. (A.4), (A.7), and (A.8))

In Eqs. (A.7), (A.8) and Eq. (A.4), the sum is over pairs (n_{pair}) for a fixed $\Delta z = \Delta z_m$ such that $|z_a - z_b| = |z_c - z_d| = \Delta z_m$. The form of the covariance of the two-point correlation function can be used to achieve the best sensitivity for the detection of neutrino mass. The following choices are possible:

- (I) $a = c$ and $b = d$. In this case, both the noise and the signal terms in Eqs. (A.7) and (A.8) contribute maximally and results in the worst possible sensitivity. We note that the signal term term dominates the spectroscopic noise term in this case for $\Delta r \lesssim 2 \text{ Mpc}$.
- (II) $a \neq c$ and $b \neq d$. In this case, the spectroscopic noise doesn't contribute but the signal term's contribution depends on the separation of pairs.
- (III) $a \neq c$ and $b \neq d$ and widely separated pairs. Under this condition $\xi_{ac}, \xi_{ad}, \xi_{bc}, \xi_{bd} \ll 1$ (Figure 1). This drives both the noise and signal terms in Eqs. (A.7) and (A.8) to very small values. If only such pairs are considered in the analysis of data, the covariance matrix becomes nearly singular. This yields a near zero-noise estimator. We consider this case in this paper and find that, for a QSO line-of-sight, the covariance matrix can be nearly independent of Δz (for details see Figure 2 and discussion in Appendix A). This allows us to express the covariance as a diagonal matrix:

$$\text{COV}(z_a, z_b; z_c, z_d) = \sigma_{\text{COV}}^2 \quad (3.2)$$

where σ_{COV} expresses the effective noise in the measurement of two-point correlation function and encompasses the impact of both the spectroscopic noise and the signal covariance.

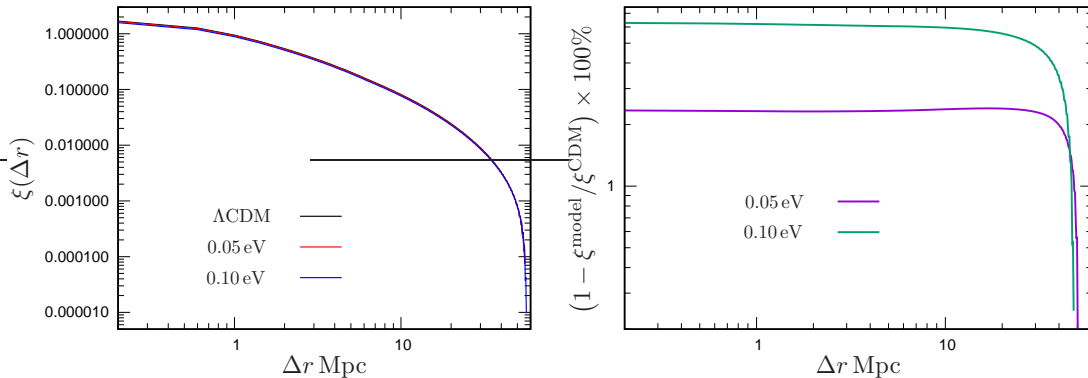


Figure 1. Left Panel: One-dimensional correlation function $\xi(\Delta r)$ (see Eq. (2.7)) is shown as a function of separation Δr for the Λ CDM model and the models with neutrino masses: $m_\nu = 0.05$ eV and $m_\nu = 0.1$ eV. Right Panel: Percentage difference of one-dimensional correlation functions $\xi(\Delta r)$ between Λ CDM model and the models with neutrino masses: $m_\nu = 0.05$ eV and $m_\nu = 0.1$ eV, as functions of separation Δr .

3.1 Choice of parameters

We choose six parameters for our analysis: three cosmological parameters: $\Omega_{\nu 0} h^2 = \sum m_\nu / (94 \text{ eV})$, $\Omega_{m 0} h^2$, the energy density of cold dark matter, and n_s , the scalar spectral index and three parameters corresponding to dynamical and thermal state of Lyman- α clouds: β , T_0 , and J_0 .

The neutrino mass $\sum m_\nu$ is given by $\Omega_{\nu 0} h^2 = \sum m_\nu / 94.22$. In addition to $\Omega_{\nu 0} h^2$, we have considered the following fiducial values of parameters for our analysis: $\Omega_{m 0} h^2 = 0.14$, $n_s = 0.9617$, $\beta = 2.21$ ($\gamma = 0.7$), $T_0 = 0.95 \times 10^4$ K, $J_0 = 1.5 \times 10^{12} \text{ s}^{-1}$. These fiducial values are based on the bestfit values of these parameters determined from Lyman- α data (for details see [8]). Our results are insensitive to the choice of these fiducial values.

While Lyman- α forest data allows probe of smaller scales ($k \simeq 5 \text{ Mpc}^{-1}$) that one exploits to determine neutrino masses, this data only probes a only small range of scales (typically between 0.5–50 Mpc) and its interpretation is harder owing to uncertainty in the ionization, thermal, and dynamical evolution of the IGM and Lyman- α clouds (e.g. [8]). As we will see below, the parameter corresponding to neutrino mass is degenerate with other cosmological parameters such as n_s and $\Omega_m h^2$, which are determined only poorly from the Lyman- α data (for details see [8]). But these parameters have been determined with great precision by CMB anisotropy measurements using Planck, which probe scales from $k \simeq 10^{-4}$ – 0.1 Mpc^{-1} (e.g. [5]). Therefore, any proposal that relies on Lyman- α data to determine neutrino masses gains from the use of prior information from CMB data.

We use Planck 1- σ error bars as priors for our analysis. We do not choose either the baryon density $\Omega_b h^2$ or the overall normalization A_s in our analysis as they do not give additional information. Planck determines A_s , which normalizes the two-point correlation function, with high precision but this parameter is degenerate with β which is not known with comparable precision [8]. The baryon density parameter determines the average density which is degenerate with J_0 (Eq. (2.3)).

Before embarking on a detailed analysis, we first attempt to establish how well the neutrino mass density can be determined in most ideal conditions. If the neutrino mass density is the only parameter then the error on determining the parameter from Fisher matrix is $\sigma_\nu = \sqrt{F_{11}^{-1}}$. If $\sum m_\nu = 0.10 \text{ eV}$ ($\Omega_{\nu 0} h^2 \simeq 10^{-3}$), and $\sigma_{\text{COV}}^2 = 10^{-5}$ (as we discuss in

detail in the appendix and Figure 2, this value of σ_{COV}^2 is a modest requirement), the error in the measurement of $\Omega_{\nu 0} h^2$ is: $\sigma_\nu = 1.4 \times 10^{-4}$. This gives the SNR of the detection: $\text{SNR} = \Omega_{\nu 0} h^2 / \sigma_\nu \simeq 7.55$ or an approximately 8- σ detection. For $\sum m_\nu = 0.05$ eV, the corresponding SNR $\simeq 3.7$.

The SNR in this ideal condition allows us to benchmark the degeneracy of the parameter $\Omega_{\nu 0} h^2$ with other parameters. We next include the other cosmological parameters in our analysis. These parameters ($\Omega_{m 0} h^2$ and n_s) have been measured by PLANCK with high precision. For a spatial flat cosmological model, $\Omega_{m 0} h^2 = 0.014240 \pm 0.00087(\sigma_m)$; $n_s = 0.9665 \pm 0.0038(\sigma_s)$ [5]. We use Planck errors on these parameters as priors on our Fisher matrix analysis. This can be achieved by modifying the diagonal terms as: $F_{mm}^{\text{Prior}} = F_{mm} + 1/\sigma_m^2$ and $F_{ss}^{\text{Prior}} = F_{ss} + 1/\sigma_s^2$; F_{mm} and F_{mm}^{Prior} being the diagonal elements of the fisher matrix for the cases of without and with prior on $\Omega_{m 0} h^2$. Similarly, F_{ss} and F_{ss}^{Prior} are the diagonal elements of the fisher matrix for the parameter n_s for the cases of without and with prior on n_s .

We invert the fisher matrix (including priors on $\Omega_{m 0} h^2$ and n_s) to determine the error on the measurement of $\Omega_{\nu 0} h^2$ for $\Omega_{\nu 0} h^2 = 0.001$. This gives us: $\sigma_\nu = \sqrt{[F]_{\nu\nu}^{-1}}$, where $[F]_{\nu\nu}^{-1}$ gives the element of the inverted fisher matrix for the parameter: $\Omega_{\nu 0} h^2$. For $\sigma_{\text{COV}}^2 = 10^{-5}$, the estimated error on the measurement of $\Omega_{\nu 0} h^2$ is: $\sigma_\nu = 1.5 \times 10^{-4}$, and this corresponds to $\text{SNR} = \Omega_{\nu 0} h^2 / \sigma_\nu \simeq 7.2$. For $\sum m_\nu = 0.05$ eV, the corresponding SNR $\simeq 3.7$. As SNR in this case is the approximately same as the previous case, it shows that Planck errors on $\Omega_{m 0} h^2$ and n_s are small enough to make the Fisher matrix diagonal-dominated such that the degeneracy of these parameters with $\Omega_{\nu 0} h^2$ doesn't play a role in its determination. In other words, after the Planck results, the determination of neutrino energy density $\Omega_{\nu 0} h^2$ is nearly independent of other cosmological parameters in a spatially flat model.

We next consider parameters related to the thermal and dynamical state of Lyman- α clouds. These parameters are: J_0 , the background photoionization intensity, T_0 , the mean IGM temperature, and β ; β is related to the adiabatic index γ via the relation $\beta = 2 - 0.7(\gamma - 1)$. These three parameters relate to the ionization and thermal history of IGM and the dynamical evolution of Lyman- α clouds in the redshift range $2 \lesssim z \lesssim 5$ (for a detailed review see e.g. [27] and references therein). The existing data suggest that the temperature of IGM is nearly constant for $z > 3.5$: $T_0 \simeq 10^4$ K. For $z \simeq 3 - 3.5$, the temperature the medium is raised by approximately a factor of 1.5 owing to the reionization of singly-ionized helium [28]. The thermal evolution of the IGM in the entire redshift range of interest to us is consistent with the hypothesis that the temperature of optically-thin photoionized primordial gas is nearly independent of the magnitude of the ionizing flux with a weak dependence on the spectral index [27, 29]. The Lyman- α forest data is consistent with the ionizing intensity J_0 remaining constant in the redshift range $2 < z < 4.2$ [30]. The equation of state parameter γ has been determined using hydrodynamical simulations and, in this paper, we adopt this parameter in the range suggested by the comparison of these simulations with Lyman- α forest data [17, 31]. More details on the acceptable range of these parameters are given in section 4 of [20].

These parameters are not determined as well as the CDM energy density or the scalar spectral index are (for details see e.g. [8]). For the purposes of our analysis, T_0 and J_0 are partially degenerate. Both J_0 and T_0 appear in the two-point correlation \mathcal{C}^{FF} through the coefficient $A^2(z)$ (Eqs. (2.4) and (2.5)) as a product $J_0^{-2} T_0^{-1.4}$, which suggests that the change in \mathcal{C}^{FF} due to the change in the parameter J_0 can be largely compensated by the change in the parameter T_0 . However, the dependence of the parameter T_0 also affects $\mathcal{C}^{FF}(\Delta z)$ through

the Jeans wavenumber k_J (Eq. (2.9)), which partially lifts this degeneracy.

We account for the degeneracies of the Lyman- α cloud modeling parameters with neutrino energy density by carrying out fisher matrix analysis with six parameters: $\Omega_{\nu 0} h^2$, J_0 , $\Omega_{m 0} h^2$ and n_s , T_0 , β . As discussed above, we use Planck priors on $\Omega_{m 0} h^2$ and n_s in the analysis. In this case, for $\Omega_{\nu 0} h^2 = 0.001$ and $\sigma_{\text{COV}}^2 = 10^{-5}$, we get $\text{SNR} = 0.4$, for a single quasar sightline. This is significant deterioration in the prospect of detection. It also clearly identifies the main obstacle in the detection of massive neutrinos using Lyman- α forest: the parameters needed to model the Lyman- α clouds are strongly degenerate with $\Omega_{\nu 0} h^2$.

To understand degeneracy between different parameters, we next consider Principal Component Analysis (PCA) of the Fisher matrix. The Fisher matrix (and its inverse) is a symmetric, positive semi-definite matrix. Therefore, it can be diagonalized by a similarity transform: $F = O^T W O$. Here O is an orthogonal matrix with unit determinant and O^T its transpose. W is a diagonal matrix whose elements $\lambda_i \geq 0$. The rows of O are the (orthonormal) eigenvectors of the Fisher matrix. Equivalently, the Fisher matrix can be expressed as outer product of eigenvectors \mathbf{A}_i , weighed by the eigenvalues, λ_i : $\mathbf{F} = \sum_i \lambda_i \mathbf{A}_i \otimes \mathbf{A}_i$. In this formalism, it is easier to discern both the hierarchy of how well the parameters are determined and their degeneracies. If there are no degeneracies between parameters, the eigenvector is dominated by one parameter and the value of the corresponding eigenvalue (after scaling by the value of the parameter) determines how well it is determined. To illustrate this, we first consider the three-parameter case discussed above. In Tables 1 and 2 we display the eigenvalues (λ_i) and eigenvectors of the Fisher matrix (for $\sum m_\nu = \{0.05, 0.10\}$ eV) that are scaled by their respective parameter values. The choice of neutrino masses allows one to distinguish between normal and inverted hierarchy as the minimum detectable mass for normal hierarchy is $m_\nu \simeq 0.05$ eV, while it is expected to be nearly two times in inverted hierarchy. We notice that eigenvectors are dominated by a single parameter in this case. For a diagonal matrix, the signal-to-noise for the corresponding parameters $\text{SNR} \simeq \sqrt{\lambda_i}$. As expected the eigenvector dominated by $\Omega_{\nu 0} h^2$ has the smallest eigenvalue. The extent of degeneracy between a pair of parameters can be gauged by the projection of the eigenvector in the direction of the other parameter, weighed by the corresponding eigenvalues. It is significant if $\lambda_1 a^2 \simeq \lambda_2$ where a is the projection of eigenvector corresponding to eigenvalue λ_1 in the direction of the eigenvector corresponding to eigenvalue λ_2 . As $\Omega_{\nu 0} h^2$ corresponds to the smallest eigenvalue, its impact on the determination of other parameters is minimal. If n_s and $\Omega_{\nu 0} h^2$ are considered together: $a = 0.00366$, $\lambda_1 = 3.71 \times 10^5$, and $\lambda_2 = 51.88$. In this case, a is small enough to ensure n_s and $\Omega_{\nu 0}$ are nearly independent of each other. Similar conclusion can be reached for other pairs of parameters. As discussed above, the outcome in this case is driven by the priors provided by highly-precise Planck determination of $\Omega_{m 0} h^2$ and n_s .

We next consider the six-parameter case. We consider two neutrino masses ($m_\nu = \{0.05, 0.1\}$ eV) The eigenvalues and eigenvectors in this case are listed in Tables 3–6 for two cases of interest ($m_\nu = \{0.05, 0.1\}$ eV) for $\sigma_{\text{COV}}^2 = 10^{-6}$ and $\sigma_{\text{COV}}^2 = 10^{-7}$. The values of σ_{COV}^2 considered are motivated by Figure 2. The structure of eigenvectors in the six parameter case is considerably more complicated as compared to the three parameter case. To understand degeneracies between different parameters we consider the projection of eigenvectors on other parameters as discussed above and analyse the degeneracy of $\Omega_{\nu 0} h^2$ with other parameters. While this doesn't provide an exhaustive understanding of all the degeneracies that impact the determination of $\Omega_{\nu 0} h^2$ as such degeneracies could occur between multiple parameters, this case, along with the analytic expression for the two-point correlation function (Eq. (2.5)),

allows us to recognize the most dominant effects. The following inferences can be drawn from the Tables: (a) the eigenvalue corresponding to the eigenvector dominated by the parameter $\Omega_{\nu 0} h^2$ is much smaller as compared to other parameters ⁴, (b) The second and the third row show the strong degeneracy between T_0 and J_0 we already discussed above (Eq. 2.5), (c) β and n_s are also strongly degenerate and it follows from the analysis of Eq. (2.5), (d) based on the projection of vectors of higher eigenvalues in the direction of the eigenvector corresponding to $\Omega_{\nu 0} h^2$ as discussed above, it can readily be determined that $\Omega_{\nu 0} h^2$ is strongly degenerate with a combination of J_0 , T_0 , and β . However, as in the three parameter case, this parameter can be determined almost independently of the other cosmological parameter after the Planck priors on those parameters are used.

We next explore the possibility of putting priors on β , T_0 , J_0 and use them for better determination of the neutrino mass. The current data doesn't allow precise determination of these parameters. We assume the following RMS errors on the parameters T_0 and β : $\sigma_T = 0.18$, and $\sigma_\beta = -0.07$ (for details see [8]). This gives only a modest improvement in the SNR of the detection of neutrino mass. The reported values of J_0 lie within a factor of 2 around $J_0 \simeq 10^{12} \text{ sec}^{-1}$ and it shows minimal evolution with redshift (see e.g. [30]). This means that the current constraints on these parameters do not allow us to improve the detection prospects of the neutrino mass. This inference is insensitive to the assumed values of these parameters for the Fisher matrix analysis.

In Table 7, we show the projected SNR for the detection of neutrinos masses. For $\sigma_{\text{COV}}^2 = 10^{-7}$, the two neutrino masses can be determined with $\text{SNR} \simeq 1.1\text{--}2.1$. As we show in Figure 2, this is the smallest value of σ_{COV}^2 achievable along a single QSO line of sight as the total comoving distance is limited to $\simeq 150 \text{ Mpc}$ in this case. This means a marginal detection of neutrino mass might be possible using data from a single line of sight. For achieving a smaller σ_{COV}^2 , we need to consider cross-correlating pairs for larger comoving distances. This can be achieved by using data from multiple QSOs, as discussed in detail in the appendix. An order of magnitude improvement in σ_{COV}^2 allows the detection of neutrinos with $\text{SNR} \simeq 3\text{--}6$ for the relevant mass range (Table 7).

We use "zero noise" estimator in our analysis (Eq. (A.8)). One limitation of such an estimator in a realistic setting is residual noise. To compute the residual noise, we simulate the two-point correlation function (N_{FF}) of the detector noise for one line of sight; we use parameters of the QSO sample studied by [21] for the simulation. We find that $N_{\text{FF}} \lesssim 10^{-10}\text{--}10^{-11}$ for separations/pairs of interest (see the discussion preceding Eq. (A.8) for detail). This is orders of magnitude smaller than the smallest signal covariance $\text{COV}_{\text{FF}} = 10^{-8}$ (Table 7) we obtain. Therefore, the impact of residual noise is not expected to be significant on the estimates of SNR quoted in the paper.

We next discuss other sources of systematic error in our analysis. One issue is the contamination of Lyman- α forest with metal lines, which reduces the amount of data for analysis (e.g. [21] for detail). Another possible source of error is residual error in continuum subtraction. As we noted above, the need of high spectral-resolution data is proposed partly to deal with this issue. Our other assumptions relate to the physical state of IGM and Lyman- α clouds. Our choice is based on the success of hydrodynamical simulations and semi-analytic models in explaining Lyman- α data (e.g. [27] for detail). We check that our results are not affected the choice of fiducial models within the range suggested by Lyman-

⁴We note that even though the noise covariance matrix is diagonal, it is not possible to scale the results for different σ_{COV}^2 because of priors. The prior information is included after assessing the impact of noise on the Lyman- α data.

α data and hydrodynamical simulations. We also assume $\tau < 1$ in our analysis. As we note above, this assumption is imperative for relating the density perturbation with flux deficit. This assumption removes some data from Lyman- α forest and renders the sampling inhomogeneous, but doesn't either bias the estimator or alters the robustness of the statistical method (e.g. [24]). A more detailed investigation of different challenges posed by these theoretical assumptions and possible observational limitations are beyond the scope of this paper.

4 Summary and Conclusions

In this paper, we have studied the feasibility of the detection of neutrino mass ($\Omega_{\nu 0} h^2$) using high spectral-resolution Lyman- α data. We consider the line-of-sight two-point correlation function for our study. Our approach adopts Fisher matrix based on semi-analytic modelling of Lyman- α clouds. We assume six parameters for our analysis: three cosmological parameters (neutrino energy density, $\Omega_{\nu 0} h^2$; CDM energy density, $\Omega_{m 0} h^2$; scalar spectral index, n_s) and three parameters to model the Lyman- α clouds: background temperature and photon intensity (T_0 and J_0) along with equation of state of the gas in the clouds, γ . The choice of these parameters is justified. The impact of precise prior information on cosmological parameters from Planck data is also taken into account. We carry out principal component analysis of the Fisher matrix to assess degeneracies between different parameters and their impact on the determination of $\Omega_{\nu 0} h^2$. Using Planck priors, we show that $\Omega_{\nu 0} h^2$ can be determined nearly independently of cosmological parameters scalar spectral index (n_s) and the energy density of the CDM component ($\Omega_{m 0} h^2$). The main stumbling block in the precise determination of $\Omega_{\nu 0} h^2$ is its degeneracy with parameters needed to model the thermal and dynamical state of Lyman- α clouds.

We compute the covariance of line-of-sight two-point correlation function, accounting for the contribution of both the spectroscopic noise and the signal. We show that it is possible to envisage a situation (the signal is dominated by small scales ($\lesssim 10$ Mpc) whereas the error on the signal comes predominantly from the large scales ($\gtrsim 50$ Mpc)), in which the covariance can be driven to very small values for both the noise and the signal for a subset of the data in a realistic setting for $z \simeq 2-3$ (e.g. the high-spectral resolution data analyzed by Day et al. [21] could be used for our study). This near 'zero noise' estimator allows for the detection of the neutrino mass in the range $m_\nu \simeq 0.05-0.1$ eV with SNR = 1.1-2.1 for a single line-of-sight. We show that, by novel analysis of data, we could increase the SNR by using multiple QSOs. In particular, this might allow us to detect the relevant range of neutrino masses with SNR = 3-6 (Table 7).

One of the outstanding aims of modern cosmology is the detection of massive neutrinos. Current cosmological constraints on massive neutrinos ($\sum m_\nu \lesssim 0.09$ eV) are stringent enough to permit either the minimal normal or the inverted hierarchy models. Currently, no single data set seems capable of this detection as CMB/Galaxy data are available at large scales whereas the maximal impact of neutrinos is on the small scales (Figure 1). High spectral-resolution Lyman- α data can probe scales suitable for this detection but it cannot precisely determine other cosmological parameters, which are degenerate with neutrino mass. One of the possible approaches to the detection is to use the prior information from large-scale CMB and/or galaxy data to the small-scale Lyman- α data. We follow this approach in this paper. We argue that with the novel analysis of the existing Lyman- α data proposed here, massive neutrinos might be detectable.

$\sigma_{\text{COV}}^2 = 10^{-5}$; Priors used: $\sigma_m = 0.00087$, $\sigma_s = 0.0038$

Eigenvalue	$\Omega_{m0}h^2$	$\Omega_{\nu0}h^2$	n_s
57.74	-0.00275	0.9998	0.00445
1.36×10^5	0.999	0.00255	-0.04378
3.84×10^5	-0.0437	-0.00457	0.999

Table 1. Table of eigenvalues (first column) and the eigenvalues (rest of the columns) of the Fisher matrix for the 3-parameter case with $\sum m_\nu = 0.05$ eV.

$\sigma_{\text{COV}}^2 = 10^{-5}$; Priors used: $\sigma_m = 0.00087$, $\sigma_s = 0.0038$

Eigenvalue	$\Omega_{m0}h^2$	$\Omega_{\nu0}h^2$	n_s
51.88	0.00201	0.9999	0.00366
1.35×10^5	0.9995	0.0019	0.029383
3.71×10^5	-0.029375	-0.00372	0.9995

Table 2. Table of eigenvalues (first column) and the eigenvalues (rest of the columns) of the Fisher matrix for the 3-parameter case with $\sum m_\nu = 0.1$ eV.

$\sigma_{\text{COV}}^2 = 10^{-7}$; Priors used: $\sigma_m = 0.00087$, $\sigma_s = 0.0038$, $\sigma_\beta = 0.07$, $\sigma_T = 0.18$

Eigenvalue	$\Omega_{m0}h^2$	$\Omega_{\nu0}h^2$	β	T_0	J_0	n_s
5.76	0.000191	0.9985	0.015882	0.015810	-0.0492	0.00118
380.62	0.0206	-0.0441	-0.2551	0.525	-0.8093	0.0402
4×10^4	-0.3043	-0.0114	0.05207	-0.7905	-0.4971	0.1799
6.1×10^4	0.125	-0.00869	-0.331	-0.1053	-0.1234	-0.920
1.8×10^5	0.9269	-0.00347	0.15	0.28	0.151	0.127
8.57×10^5	0.178	0.0278	-0.894	-0.0955	0.238	-0.318

Table 3. Table of eigenvalues (first column) and the eigenvalues (rest of the columns) of the Fisher matrix for the 6-parameter case with $\sum m_\nu = 0.05$ eV.

$\sigma_{\text{COV}}^2 = 10^{-7}$; Priors used: $\sigma_m = 0.00087$, $\sigma_s = 0.0038$, $\sigma_\beta = 0.07$, $\sigma_T = 0.18$

Eigenvalue	$\Omega_{m0}h^2$	$\Omega_{\nu0}h^2$	β	T_0	J_0	n_s
4.69	0.00016	0.998	0.0154	0.0246	-0.0552	0.00745
1503.9	0.00411	-0.0519	-0.2644	0.62	-0.736	0.0224
3.3×10^4	-0.2674	-0.01357	0.0823	0.7436	0.597	-0.1048
5.98×10^4	0.0956	-0.00982	0.32	-0.0381	-0.117	-0.9342
1.74×10^5	0.9455	-0.00187	0.142	0.226	0.141	0.118
6.26×10^6	0.158	0.03025	-0.8945	-0.0921	0.2521	-0.3187

Table 4. Table of eigenvalues (first column) and the eigenvalues (rest of the columns) of the Fisher matrix for the 6-parameter case with $\sum m_\nu = 0.1$ eV.

The main takeaways of our analysis are: (a) it is possible to construct a near-zero noise estimator to extract cosmological information from the Lyman- α data, (b) one important application of such an estimator is to detect still-elusive massive neutrinos from these data, (c) such a detection might be possible with a small number of QSOs with high spectral-resolution (e.g. the sample of [21]).

$\sigma_{\text{COV}}^2 = 10^{-6}$; Priors used: $\sigma_m = 0.00087$, $\sigma_s = 0.0038$, $\sigma_\beta = 0.07$, $\sigma_T = 0.18$

Eigenvalue	$\Omega_{m0}h^2$	$\Omega_{\nu 0}h^2$	β	T_0	J_0	n_s
0.792	0.0000252	0.9981	0.01388	0.02034	-0.0559	0.0001487
467.39	0.00235	-0.052	-0.269	0.533	-0.8004	-0.00523
5408.15	0.0326	-0.0125	-0.0518	-0.838	-0.54	0.0107
5.71×10^4	-0.0521	0.0102	-0.341	-0.027	0.0899	0.9336
1.33×10^5	0.9768	-0.00469	0.169	0.045	-0.0246	0.1202
8.68×10^5	0.205	0.0274	-0.8827	-0.0941	0.235	-0.337

Table 5. Table of eigenvalues (first column) and the eigenvalues (rest of the columns) of the Fisher matrix for the 6-parameter case with $\sum m_\nu = 0.05$ eV.

$\sigma_{\text{COV}}^2 = 10^{-6}$; Priors used: $\sigma_m = 0.00087$, $\sigma_s = 0.0038$, $\sigma_\beta = 0.07$, $\sigma_T = 0.18$

Eigenvalue	$\Omega_{m0}h^2$	$\Omega_{\nu 0}h^2$	β	T_0	J_0	n_s
0.623	0.0000205	0.9971	0.0114	0.0339	-0.0665	0.0000972
229.21	0.000617	-0.0669	-0.27	0.622	-0.731	-0.00351
4326.92	0.0285	-0.0141	-0.0932	-0.775	-0.623	0.00773
5.7×10^4	-0.0471	-0.0113	-0.344	-0.0292	0.097	0.932
1.33×10^5	0.979	-0.00488	0.159	0.0385	-0.0255	0.1125
6.37×10^5	0.193	0.0297	-0.879	-0.0903	0.2477	-0.344

Table 6. Table of eigenvalues (first column) and the eigenvalues (rest of the columns) of the Fisher matrix for the 6-parameter case with $\sum m_\nu = 0.1$ eV.

σ_{COV}^2	$\sum m_\nu = 0.05$ eV	$\sum m_\nu = 0.1$ eV
10^{-6}	0.4	0.8
10^{-7}	1.1	2.1
10^{-8}	3.2	6.2

Table 7. The table shows the projected SNR for measuring different two neutrino masses considered here for different values of σ_{COV}^2 .

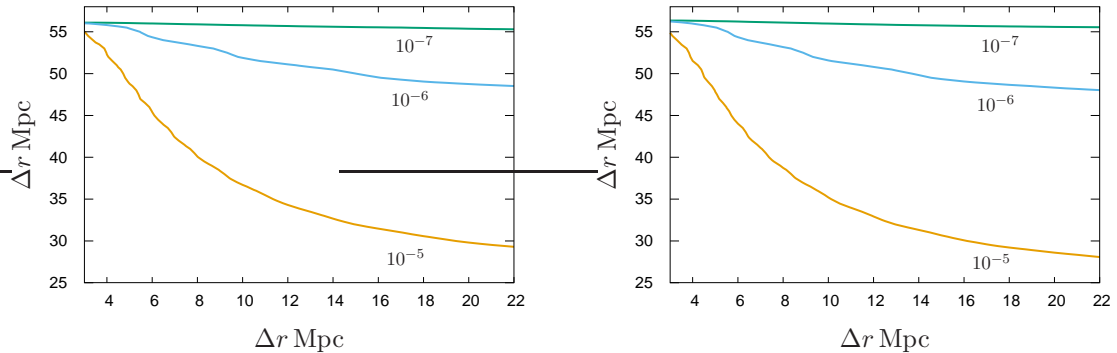


Figure 2. Contours of fixed σ_{COV}^2 (Eqs. (3.2) and (A.7)) are shown for $\sum m_\nu = 0.05$ eV (left panel) and $\sum m_\nu = 0.1$ eV (right panel). Each curve is labelled by a σ_{COV}^2 value which is computed using Eq. (A.7).

A Appendix A: Covariance of the Estimator

The starting point of computing the covariance of the two-point function is to define the unbiased estimator of the two-point function of the flux contrast:

$$\hat{E}_{FF}(z_a, z_b) = \frac{1}{n_{\text{pair}}} \sum_{a=1}^{n_{\text{pair}}} \delta_F(z_a) \delta_F(z_b) \quad (\text{A.1})$$

Here $z_b = z_a + \Delta z_{ab}$ and n_{pair} is the number of redshift pairs that correspond to the same redshift separation Δz_{ab} ⁵. The flux contrast $\delta_F(z_a)$ receives contribution from both the signal and spectroscopic noise. Assuming the signal and noise to be uncorrelated, we get:

$$\delta_F(z_a) \delta_F(z_b) = \hat{C}_{FF}(z_a, z_b) + \hat{N}_{FF}(z_a, z_b) \quad (\text{A.2})$$

Here $\hat{C}_{FF}(z_a, z_b)$ and $\hat{N}_{FF}(z_a, z_b)$ correspond to the signal and the spectroscopic noise, respectively.

$$\langle \hat{N}_{FF}(z_a, z_b) \rangle = \sigma_N^2 \delta_{a,b}, \quad (\text{A.3})$$

This defines σ_N^2 , the variance of the spectroscopic noise. The covariance of the estimator given by Eq. (A.1) can be expressed as:

$$\begin{aligned} \text{COV}(z_a, z_b; z_c, z_d) &= \left\langle \left[\hat{E}_{FF}(z_a, z_b) - E_{FF}(z_a, z_b) \right] \left[\hat{E}_{FF}(z_c, z_d) - E_{FF}(z_c, z_d) \right] \right\rangle \\ &= \langle \hat{C}_{FF}(z_a, z_b) \hat{C}_{FF}(z_c, z_d) \rangle - C_{FF}(z_a, z_b) C_{FF}(z_c, z_d) + \\ &\quad \langle \hat{N}_{FF}(z_a, z_b) \hat{N}_{FF}(z_c, z_d) \rangle - \sigma_N^4 \delta_{a,b} \delta_{c,d}. \end{aligned} \quad (\text{A.4})$$

where $E_{FF}(z_a, z_b) = \langle \hat{E}_{FF}(z_a, z_b) \rangle$, and we have used the fact that the estimator for the Lyman- α forest and that for the noise are uncorrelated:

$$\begin{aligned} \left\langle \hat{C}_{FF}(z_a, z_b) \hat{N}_{FF}(z_c, z_d) \right\rangle &= \left\langle \hat{C}_{FF}(z_a, z_b) \right\rangle \left\langle \hat{N}_{FF}(z_c, z_d) \right\rangle \\ &= C_{FF}(z_a, z_b) \sigma_N^2 \delta_{c,d} \end{aligned} \quad (\text{A.5})$$

Eq. (A.4) requires us to compute the expectation value of both the signal and noise four-point functions. It can be shown that:

$$\begin{aligned} \left\langle \hat{C}_{FF}(z_a, z_b) \hat{C}_{FF}(z_c, z_d) \right\rangle &= \langle \delta_b(z_a) \delta_b(z_b) \delta_b(z_c) \delta_b(z_d) \rangle \\ &= A^4 \times e^{-2\beta\xi(0)} \times e^{\frac{\beta^2}{2} \langle (\delta_b(z_a) + \delta_b(z_b) + \delta_b(z_c) + \delta_b(z_d))^2 \rangle} \\ &= A^4 \times e^{2(\beta^2 - \beta)\xi(0)} \times e^{\beta^2 (\xi_{ab} + \xi_{cd} + \xi_{ac} + \xi_{ad} + \xi_{bd} + \xi_{bc})} \end{aligned} \quad (\text{A.6})$$

It further follows that:

$$\begin{aligned} &\left\langle \hat{C}_{FF}(z_a, z_b) \hat{C}_{FF}(z_c, z_d) \right\rangle - C_{FF}(z_a, z_b) C_{FF}(z_c, z_d) \\ &= A^4 \times e^{2(\beta^2 - \beta)\xi(0)} \times e^{\beta^2 (\xi_{ab} + \xi_{cd})} \times \left[e^{\beta^2 (\xi_{ac} + \xi_{ad} + \xi_{bd} + \xi_{bc})} - 1 \right] \end{aligned} \quad (\text{A.7})$$

⁵The number of pairs could get contribution not only from one line of sight but from multiple QSOs along different line of sights

Eq. (A.7) yields the relevant expression for the signal terms in Eq. (A.4). We next consider the noise terms. It can be shown that:

$$\begin{aligned}
& \frac{1}{n_{\text{pair}}^2} \left[\sum_{a,c=1}^{n_{\text{pair}}} \left\langle \hat{N}_{FF}(z_a, z_a + \Delta z_{ab}) \hat{N}_{FF}(z_c, z_c + \Delta z_{cd}) \right\rangle \right] - \sigma_N^4 \delta_{ab} \delta_{cd} \\
&= \frac{1}{n_{\text{pair}}^2} \sum_{a,c=1}^{n_{\text{pair}}} [\sigma_N^4 (\delta_{ac} \delta_{bd} + \delta_{ad} \delta_{bc})] \\
&= \frac{2\sigma_N^4}{n_{\text{pair}}} \quad \text{for } \Delta z_{ac}, \Delta z_{ad}, \Delta z_{bc}, \Delta z_{bd} = 0 \\
&= \frac{\sigma_N^4}{n_{\text{pair}}} \quad \text{for } \Delta z_{ac}, \Delta z_{bd} = 0 \\
&= 0 \quad \text{otherwise,}
\end{aligned} \tag{A.8}$$

Eqs. (A.7) and (A.8) provide both the signal and the spectroscopic noise terms in the covariance of the two-point function (Eq. (A.4)).

It should be noted that the noise contribution declines as $1/n_{\text{pair}}$. n_{pair} can be increased by considering lines of sights to multiple QSOs. The signal contribution in the covariance (Eq. (A.7)) can also be decreased by considering multiple lines of sights but that process is more complicated and is discussed below. It should be further noted that if $z_a \neq z_b \neq z_c \neq z_d$ the spectroscopic noise term (Eq. (A.8)) is driven to zero. In other words, if two different redshift pairs are used for the Fisher matrix analysis, the covariance might receive contribution from only the signal covariance. We simulate the contribution of the noise using the parameters of Day et al. [21] sample, and verify that, for our proposed method of analysis, the covariance of the two-point function is dominated by the signal. It also follows from Eq. (A.7) that if the pairs are widely separated, the signal contribution can also be reduced by a large amount as the one-dimensional correlation function for widely separated points fall very rapidly (Figure 1). In Figure 2 we show contours of a fixed $\text{COV}(z_a, z_b; z_c, z_d)$ using Eq. (A.7), in the limit when the separation between the two pairs is much larger than the intra-pair separation. The x-axis corresponds to the intra-pair separation while the y-axis correspond to the separation between two pairs. It is clear σ_{COV}^2 falls sharply for large inter-pair separation and reaches a nearly constant value when the separation between pairs approaches distances $\simeq 60$ Mpc or so. This motivates us to consider nearly constant σ_{COV}^2 in the foregoing. We further note that contours shown in Figure 2 are suitable for a single QSO line of sight of (comoving) length $\simeq 150$ Mpc. In such a case, the separation of pairs cannot exceed $\simeq 100$ Mpc, which puts a lower limit on the value of σ_{COV}^2 .

However, if we consider multiple QSO lines of sights, σ_{COV}^2 can be decreased further. This can be understood by analyzing the structure of Eq. (A.7) by considering two QSOs. The two small-scale pairs (ab and cd) may correspond to the line of sights of each of the QSOs while the cross-correlation on large scales (ac , ad , etc.) is carried out between the different QSOs. Eqs. (2.7) and (2.8) have to be suitably modified for this case. Eq. (2.8) is derived along a given direction by fixing the other two coordinates (e.g. [32] for details). Since the power spectrum is rotationally invariant, eq. (2.8) is left unchanged by rotating the axis such that it connects two points on different QSOs. Similarly, Eq. (2.7) can be cast in terms of the comoving distance between two points rather than just the redshift difference. We note that when the comoving distance is larger than a few hundred Mpc, it is possible to achieve

$\sigma_{\text{COV}}^2 \simeq 10^{-8}$ (Table 7). We find that simultaneous analysis based around 10 QSOs in the redshift range $z \simeq 2\text{--}2.5$ could achieve our proposed outcome (e.g. the sample studied by [21]).

Acknowledgements

AKS would like to acknowledge the financial aid and computational resources provided by the National Centre for Radio Astrophysics, Tata Institute of Fundamental Research, Pune under their regular institute Post - Doctoral Fellow program.

References

- [1] S. Ahmed, A. Anthony, E. Beier, A. Bellerive, S. Biller, J. Boger et al., *Measurement of the total active b 8 solar neutrino flux at the sudbury neutrino observatory with enhanced neutral current sensitivity*, *Physical review letters* **92** (2004) 181301.
- [2] P. Adamson, C. Andreopoulos, K. Arms, R. Armstrong, D. Auty, D. Ayres et al., *Measurement of neutrino oscillations with the minos detectors in the numi beam*, *Physical Review Letters* **101** (2008) 131802.
- [3] S. Abe, T. Ebihara, S. Enomoto, K. Furuno, Y. Gando, K. Ichimura et al., *Precision measurement of neutrino oscillation parameters with kamland*, *Physical review letters* **100** (2008) 221803.
- [4] M.S. Athar, S.W. Barwick, T. Brunner, J. Cao, M. Danilov, K. Inoue et al., *Status and perspectives of neutrino physics*, *Progress in Particle and Nuclear Physics* **124** (2022) 103947.
- [5] N. Aghanim, Y. Akrami, M. Ashdown, J. Aumont, C. Baccigalupi, M. Ballardini et al., *Planck 2018 results-vi. cosmological parameters*, *Astronomy & Astrophysics* **641** (2020) A6.
- [6] E. Di Valentino, S. Gariazzo and O. Mena, *Most constraining cosmological neutrino mass bounds*, *Physical Review D* **104** (2021) 083504.
- [7] C. Yèche, N. Palanque-Delabrouille, J. Baur and H.D.M. Des Bourboux, *Constraints on neutrino masses from lyman-alpha forest power spectrum with boss and xq-100*, *Journal of Cosmology and Astroparticle Physics* **2017** (2017) 047.
- [8] N. Palanque-Delabrouille, C. Yèche, N. Schöneberg, J. Lesgourgues, M. Walther, S. Chabanier et al., *Hints, neutrino bounds, and wdm constraints from sdss dr14 lyman- α and planck full-survey data*, *Journal of Cosmology and Astroparticle Physics* **2020** (2020) 038.
- [9] C.T. Pedersen, *Neutrino mass and cosmology from the Lyman-alpha forest*, Ph.D. thesis, UCL (University College London), 2021.
- [10] G. Rossi, N. Palanque-Delabrouille, A. Borde, M. Viel, C. Yèche, J.S. Bolton et al., *Suite of hydrodynamical simulations for the lyman- α forest with massive neutrinos*, *Astronomy & Astrophysics* **567** (2014) A79.
- [11] N. Palanque-Delabrouille, C. Yèche, J. Baur, C. Magneville, G. Rossi, J. Lesgourgues et al., *Neutrino masses and cosmology with lyman-alpha forest power spectrum*, *Journal of Cosmology and Astroparticle Physics* **2015** (2015) 011.
- [12] S. Gratton, A. Lewis and G. Efstathiou, *Prospects for constraining neutrino mass using planck and lyman- α forest data*, *Physical Review D* **77** (2008) 083507.
- [13] M. Gerbino and M. Lattanzi, *Status of neutrino properties and future prospects—cosmological and astrophysical constraints*, *Frontiers in Physics* **5** (2018) 70.
- [14] M. Rauch, *The lyman alpha forest in the spectra of quasistellar objects*, *Annual Review of Astronomy and Astrophysics* **36** (1998) 267.

- [15] P. Coles and B. Jones, *A lognormal model for the cosmological mass distribution*, *Monthly Notices of the Royal Astronomical Society* **248** (1991) 1.
- [16] H. Bi and A.F. Davidsen, *Evolution of structure in the intergalactic medium and the nature of the Ly α forest*, *The Astrophysical Journal* **479** (1997) 523.
- [17] L. Hui and N.Y. Gnedin, *Equation of state of the photoionized intergalactic medium*, *Monthly Notices of the Royal Astronomical Society* **292** (1997) 27.
- [18] T.R. Choudhury, R. Srianand and T. Padmanabhan, *Semianalytic approach to understanding the distribution of neutral hydrogen in the universe: comparison of simulations with observations*, *The Astrophysical Journal* **559** (2001) 29.
- [19] K.L. Pandey and S.K. Sethi, *Probing primordial magnetic fields using Ly α clouds*, *The Astrophysical Journal* **762** (2012) 15.
- [20] A.K. Sarkar, K.L. Pandey and S.K. Sethi, *Using the redshift evolution of the Lyman- α effective opacity as a probe of dark matter models*, *Journal of Cosmology and Astroparticle Physics* **2021** (2021) 077.
- [21] A. Day, D. Tytler and B. Kambalur, *Power spectrum of the flux in the Lyman-alpha forest from high-resolution spectra of 87 quasars*, *Monthly Notices of the Royal Astronomical Society* **489** (2019) 2536.
- [22] C.-A. Faucher-Giguère, J. Prochaska, A. Lidz, L. Hernquist and M. Zaldarriaga, *A direct precision measurement of the intergalactic Lyman- α opacity at $2 \leq z \leq 4.2$* , *Nuovo Cimento B Serie* **122** (2007) 1249.
- [23] S. Chatterjee, K.M.A. Elahi, S. Bharadwaj, S. Sarkar, S. Choudhuri, S. Sethi et al., *The Tracking Tapered Gridded Estimator for the 21-cm power spectrum from MWA drift scan observations I: Validation and preliminary results*, *arXiv e-prints* (2024) [arXiv:2405.10080 \[2405.10080\]](https://arxiv.org/abs/2405.10080).
- [24] A.K. Patwa, S. Sethi and K.S. Dwarakanath, *Extracting the 21 cm EoR signal using MWA drift scan data*, *Monthly Notices of the Royal Astronomical Society* **504** (2021) 2062 [<https://academic.oup.com/mnras/article-pdf/504/2/2062/37518347/stab989.pdf>].
- [25] D.J. Eisenstein and W. Hu, *Power spectra for cold dark matter and its variants*, *The Astrophysical Journal* **511** (1999) 5.
- [26] D. Sivia and J. Skilling, *Data analysis: a Bayesian tutorial*, OUP Oxford (2006).
- [27] M. McQuinn, *The evolution of the intergalactic medium*, *Annual Review of Astronomy and Astrophysics* **54** (2016) 313.
- [28] P. La Plante, H. Trac, R. Croft and R. Cen, *Helium reionization simulations. iii. the helium Ly α forest*, *The Astrophysical Journal* **868** (2018) 106.
- [29] B.T. Draine, *Physics of the interstellar and intergalactic medium*, vol. 19, Princeton University Press (2010).
- [30] C.-A. Faucher-Giguere, A. Lidz, L. Hernquist and M. Zaldarriaga, *A flat photoionization rate at $2 \leq z \leq 4.2$: Evidence for a stellar-dominated UV background and against a decline of cosmic star formation beyond $z \sim 3$* , *The Astrophysical Journal* **682** (2008) L9.
- [31] Z. Lukić, C.W. Stark, P. Nugent, M. White, A.A. Meiksin and A. Almgren, *The Lyman α forest in optically thin hydrodynamical simulations*, *Monthly Notices of the Royal Astronomical Society* **446** (2015) 3697.
- [32] V. Desjacques and A. Nusser, *Redshift distortions in one-dimensional power spectra*, *Monthly Notices of the Royal Astronomical Society* **351** (2004) 1395.